THE JOURNAL OF BIOLOGICAL CHEMISTRY VOL. 287, NO. 12, pp. 8782–8791, March 16, 2012

Function of Transient Receptor Potential Cation Channel Subfamily V Member 4 (TRPV4) as a Mechanical Transducer in Flow-sensitive Segments of Renal Collecting Duct System*

Received for publication, Received September 27, 2011, and in revised form, January 30, 2012 Published, JBC Papers in Press, February 1, 2012, DOI 10.1074/jbc.M111.308411

Jonathan Berrout[1], **Min Jin**[1], **Mykola Mamenko, Oleg Zaika, Oleh Pochynyuk, and Roger G. O'Neil**[2]

From the Department of Integrative Biology and Pharmacology, The University of Texas Health Science Center, Houston, Texas 77030

Background: TRPV4 is a Ca^{2+}-permeable channel that is expressed in a wide range of cells and tissues.
Results: TRPV4 is expressed in renal connecting tubule/collecting duct cells and is activated by fluid flow.
Conclusion: TRPV4 is critical as a flow transducer in the mammalian collecting duct system.
Significance: TRV4 may underlie mechanically sensitive phenomena in the distal nephron.

The TRPV4 Ca^{2+}-permeable channel is sensitive to mechanical stimuli. In the current study we have employed immunocytochemical staining in kidney slices and functional assessments (Ca^{2+} imaging) in isolated, split-opened, tubule segments to define TRPV4 sites of expression and flow-dependent function in the collecting duct system. Staining patterns revealed strong expression of TRPV4 along the entire collecting duct system with highest levels at the apical (luminal)/subapical region of the principal cells (PCs), the dominant cell type, with more diffuse staining in intercalated cells (ICs). Using fluorescence Ca^{2+} imaging and the selective TRPV4 agonist, GSK1016790A, we demonstrated functional TRPV4 channels in PCs and ICs of split-opened cortical collecting ducts and connecting tubules. The agonist was ineffective in inducing a rise in $[Ca^{2+}]_i$ in the absence of extracellular Ca^{2+} or in tubules from TRPV4-deficient animals. Most importantly, a 10-fold elevation in luminal (apical) fluid flow induced a rapid and sustained influx of Ca^{2+} that was abolished by the TRPV channel inhibitor, ruthenium red, or in tubules isolated from TRPV4 deficient animals. We concluded that TRPV4 is highly expressed along the entire collecting duct system where it appears to function as a sensor/transducer of flow-induce mechanical stresses.

TRPV4[3] is a Ca^{2+}-permeable cation channel that is widely expressed in both excitable and nonexcitable cells. Although the TRPV4 channel can be activated by a wide range of stimuli, it has been shown to be particularly sensitive to physical alterations of the cellular microenvironment as it can be activated by variations in osmolality (1, 2), fluid shear stress/flow (3–6), pressure (7), and moderate heat (8, 9). Hence, it is becoming evident that the channel may play a critical role in sensing and/or transducing changes in the microenvironmental physical state, at least in some cells.

TRPV4 is known to be expressed in the kidney (2). Although it has been anticipated that the channel likely functions to regulate some aspects of fluid and electrolyte balance, it remains perplexing that animals deficient in the *TRPV4* gene do not display particularly noted changes in fluid and electrolyte excretion patterns (10). Recent studies, however, point to an apparent role of TRPV4 as a sensor of fluid shear stress or fluid flow in renal cells and tissues. Indeed, our laboratory recently demonstrated that endogenous TRPV4 in M-1 collecting duct cells is activated by increases in shear stress/fluid flow, a response that is abolished following siRNA knockdown of TRPV4 (3, 4). Furthermore, Suzuki and co-workers (14) have shown that flow-dependent K^+ secretion, a Ca^{2+}-dependent process utilizing the maxi-K channel (11–13), is essentially abolished in TRPV4 knock-out animals. These results are consistent with earlier studies demonstrating that elevated flows in both the isolated perfused connecting tubule (CNT) and the immediate downstream segment, the cortical collecting duct (CCD), display flow-induced activation of Ca^{2+} signaling and/or activation of luminal Ca^{2+}-permeable channels (15, 16). Hence, it may be that TRPV4 plays a central role in flow-dependent phenomena in the late distal tubule and collecting duct.

The purpose of the present study was to elucidate the sites of expression and potential function of TRPV4 as a flow sensor/transducer in the mouse collecting duct system. We show that TRPV4 is expressed along the entire length of the collecting duct system, from CNT to papillary collecting duct, with prominent expression near the luminal (apical) border of aquaporin-2-expressing principal cells (PCs) and less pronounced expression levels in intercalated cells (ICs). Further, Ca^{2+} imaging studies in isolated split-opened CNT and CCD preparations demonstrated specific activation of TRPV4 by the TRPV4 agonist GSK1016790A in all cells. Most importantly, high flow rates over the luminal surface led to a rapid and sustained influx

* The study was supported, in whole or in part, by National Institutes of Health Grants R01 DK070950 (to R. G. O.) and R21 DE018522 (to R. G. O.). This work was also supported by American Heart Association Grant SDG2230391 (to O. P.) and the Carl W. Gottschalk Research Scholar Grant from the American Society of Nephrology (to O. P.).
[1] Both authors contributed equally to this work.
[2] To whom correspondence should be addressed: Dept. of Integrative Biology and Pharmacology, The University of Texas Health Science Center, 6431 Fannin St., Rm. MSB 4.132, Houston, TX 77030. Tel.: 713-500-6316; Fax: 713-500-7444; E-mail: roger.g.oneil@uth.tmc.edu.
[3] The abbreviations used are: TRPV4, transient receptor potential cation channel subfamily V member 4; AQP2, aquaporin-2; CCD, cortical collecting duct; CNT, connecting tubule; DCT, distal convoluted tubule; HEK, human embryonic kidney; IC, intercalated cell; NCX, Na^+:Ca^{2+} exchanger; PC, principal cell; PNA, peanut agglutinin; SS, shear stress.

of Ca^{2+} into both PCs and ICs, a response that was abolished in tubules isolated from animals deficient in the *TRPV4* gene. It is concluded that TRPV4 is expressed in the collecting duct system where this channel appears to function as a central component of a flow-sensor/transducer in these cells.

EXPERIMENTAL PROCEDURES

Isolation and Preparation of Split-opened Kidney Tubules—Segments of CCD and CNT were isolated and prepared from mouse kidney tissue as described previously (17, 18). Briefly, mice were sacrificed by CO_2 administration and immediately subjected to cervical dislocation (the protocol was approved by the Institute for Animal Care and Use Committee of The University of Texas Health Science Center). Kidneys were immediately removed, cut into transverse sections (~1 mm thick), and placed in ice-cold PBS buffered with HEPES, pH 7.4. Medullary-cortical strips of tubules were first pulled free from the slices with watchmaker forceps and then individual CCD dissected free from surrounding tissue in the mid to upper cortical area under stereomicroscopic examination. Sites of bifurcation of the CCD were used to identify upstream CNT that merge into the CCD. Isolated tubules were moved onto 5 × 5-mm coverslip glass chips coated with poly-L-lysine for attachment. The glass coverslips with attached tubules were then placed on a perfusion chamber mounted on the stage of an inverted Nikon microscope (Eclipse Ti) and the tubule segments split-open with two sharpened micropipettes, each attached to micromanipulators. The split-opened tubules would roll out, flatten, and attach to the treated coverslip allowing direct access to the apical (luminal) border of the cells. The tubule fragments were then loaded with fura-2 and used within 1–2 h of isolation.

Immunocytochemistry of Kidney Tissue—Standard immunohistochemical procedures were utilized for evaluating TRPV4 expression sites in sections of mouse kidney. Briefly, animals were anesthetized by isoflurane inhalation and kidneys prepared by intracardiac perfusion with a clearing solution (20 ml, 0.1 M cacodylate buffer and 4% hydroxyethyl starch in ice-cold PBS, pH 7.4) followed immediately by a fixation solution (20 ml, 4% paraformaldehyde and 0.1 M cacodylate buffer in ice-cold PBS, pH 7.4). Kidneys were removed and placed in 4% paraformaldehyde overnight, then mounted in tissue freezing medium (Tissue Tek) and frozen at −30 °C. Either sagittal or transverse sections (typically 30 μm thick) were obtained, using an OTF 5000 cryostat (Bright Instrument). Sections were allowed to warm to room temperature and washed in PBS. Sections were then blocked with 1% donkey serum and incubated overnight at 4 °C with primary antibody: anti-TRPV4 (1:500; Alomone), anti-AQP2 tagged with ATTO 550 (1:200; Alomone), anti-NCX (Na^+:Ca^{2+} exchanger, 1:500; Swant). Sections were subsequently washed and incubated at room temperature for 3 h with secondary antibody: Cy2 anti-rabbit (1:100–500 Jackson ImmunoResearch) and Cy5 anti-mouse (1:500, Jackson ImmunoResearch). The tissue was then mounted with VectaShield mounting medium (Vector Laboratories) and imaged with a Nikon A1 confocal microscope in a manner similar to that used before (3, 4).

Split-opened CCD tubules were isolated and prepared as described above. Tubules on coverslip chips were fixed with 4% paraformaldehyde for 20 min at room temperature, blocked with 1% donkey serum, then incubated with primary antibodies anti-TRPV4 (1:500; Alomone) and anti-AQP2 tagged with ATTO 550 for 3 h at room temperature. Subsequently, tubules were treated with secondary antibody Cy2 anti-rabbit and fluorescein-labeled peanut agglutinin (PNA, 1:1000; Vector Laboratories), an IC marker, for 1–2 h at room temperature. Images were acquired using a Nikon A1 confocal microscope, and measurement of fluorescent intensity was performed with NIS Elements imaging software.

Measurement of Intracellular Calcium—Ratiometric fluorescence imaging of fura-2 was used to monitor intracellular calcium levels, $[Ca^{2+}rsqb]_i$, in split-opened tubule preparations using standard procedures as done extensively before (4, 17, 19). Briefly, tubule fragments on coverslip chips were loaded with fura-2/AM (2 μM) for 40 min, washed, placed on the coverslip bottom of an open perfusion chamber (0.5 ml), and imaged with a InCa Imaging Work station (Intracellular Imaging, Inc.) at 37 °C using a 20× Nikon Super Fluor objective. $[Ca^{2+}]_i$ was estimated from the fura-2 fluorescence by excitation at 340 nm and 380 nm and calculating the ratio of the emission intensities at 511 nm in the usual manner every 5 s. Results are presented as the emission ratios and denoted F_{340}/F_{380}. In some studies cells were subjected to intracellular fura-2 calibration and the ratios converted to intracellular calcium activity as described by Grynkiewicz *et al.* (20) using methods outlined previously (3, 4). For each treatment group, from 3 to 6 split-opened tubule preparations were typically utilized from which 5–12 cells were assessed for $[Ca^{2+}]_i$ levels. The data are typically presented as total number of cells analyzed for each treatment group.

Flow Rate Protocols—Split-opened tubules were typically studied in a control isotonic medium containing 150 mM NaCl, 5 mM KCl, 2 mM $MgCl_2$, 1 mM $CaCl_2$, 10 mM HEPES, and 5 mM glucose at pH 7.4. Medium with 0 Ca^{2+} was identical except $CaCl_2$ was removed and replaced with 1 mM EGTA in the control solution. To test the effect of elevating fluid flow rate over the split-opened tubule, the normal perfusion rate through the chamber (volume ~0.5 ml) was rapidly switched from the control flow rate of 1.5 ml/min (control flow rate) to 15 ml/min (high flow rate) with the gravity-feed perfusion system. Because this was done in an open chamber fluid shear stress could not be calculated because unstirred layers would be present and laminar flow may not be achieved.

In some studies, the effect of fluid shear stress on $[Ca^{2+}]_i$ was evaluated directly. Shear stress in the collecting duct system can range from <0.5 dyne/cm^2 to >20 dynes/cm^2 with typical values near 1–10 dynes/cm^2 (see Refs. 4, 26). To evaluate the response of our split-opened tubule to "physiological" shear stress (1 and 3 dynes/cm^2), we performed a few experiments in fura-2-loaded split-opened CCDs studied in a parallel plate chamber (LFR-25 chamber; C & L Instruments). Split-opened tubules were attached to the bottom coverslip (poly-L-lysine-coated) of a parallel plate chamber and placed on an inverted microscope which allowed monitoring of $[Ca^{2+}]_i$ as described previously (see Refs. 4, 41). Flow rates through the chamber were controlled by a peristaltic pump to set the shear stress level.

Chemicals—The following drugs and chemicals were used in the study: GSK1016790A (GSK101; Santa Cruz Biotechnology, stock solution, 10 μM in dimethyl sulfoxide), ruthenium red (RuR; Sigma-Aldrich, in PBS), and EGTA (Sigma).

Data are presented as mean values ± S.E. Student's *t* test or ANOVA was used to test for statistical significance, as appropriate, with $p < 0.05$ considered significant.

RESULTS

Identification of TRPV4 Sites of Expression—To identify the sites of expression of TRPV4 in the collecting duct system, mouse kidney sections were immunostained for TRPV4, AQP2 (a marker of PCs), and NCX (Na^+:Ca^{2+} exchanger, a marker of the immediate upstream segment of the CNT, the distal convoluted tubule (DCT)) (21, 22). As shown in the thick sections (30 μm) in Fig. 1*A*, TRPV4 was strongly expressed in both the cortex and medulla. However, staining was restricted to the AQP2-positive segments throughout the medulla and cortex. No TRPV4 staining was observed in the earlier nephron segments from glomerulus to DCT. An expanded view of the outer cortex revealed strong staining in both the CNT and CCD as shown in Fig. 1*B*. The figure shows a bifurcated AQP2-positive segment reflecting two CNTs merging into one CCD. As is apparent, TRPV4 was expressed in both segments and displayed strong co-localization with AQP2, reflecting the PC, as demonstrated by the merged image (Fig. 1*B*, *Merge*). In addition, a few cells in the merged image stained lightly for TRPV4, but not AQP2, as evident by the *green* pattern of staining, reflecting localization of TRPV4 in ICs. Further, in an outer cortical view of an apparent CNT (weak NCX staining, AQP2-positive), an adjacent DCT was identified by the strong NCX-positive and AQP2-negative staining (Fig. 1*C*), but did not show any evidence of TRPV4 expression.

To verify the TRPV4 specificity of our antibody for TRPV4, in separate studies we have demonstrated that our antibody (directed at the C terminus, Alomone Laboratory anti-TRPV4) recognized an appropriate double band (~100 kDa) for TRPV4 in TRPV4-transfected HEK cells, but not in nontransfected HEK cells (19). Immunocytochemistry and functional assays confirmed identification of TRPV4 only in the TRPV4-expressing cells. Further, in a separate study, a previously characterized second anti-TRPV4 antibody targeting the N terminus of TRPV4 was used to stain mouse kidney thin sections (5 μm) (4). Using a thin section, strong anti-TRPV4 binding of this second antibody was apparent along the luminal border of a CCD as shown in Fig. 1*B* (*Inset*). Finally, in kidney sections from TRPV4 knock-out animals no apparent anti-TRPV4 binding was detected (Fig. 1*D*). Hence, TRPV4 expression appears to be limited to all AQP2-positive segments of the collecting duct system.

Functional Assessment of TRPV4 Expression—To provide a functional assessment of TRPV4 in the collecting duct system, CNT and CCD tubule segments were hand-dissected and split open to gain access to the luminal cell border as done before (17, 18, 23). Using fluorescence ratiometric imaging of the Ca^{2+}-sensitive probe, fura-2, $[Ca^{2+}]_i$ was monitored and presented as the ratio F_{340}/F_{380} (or $[Ca^{2+}]_i$ in summary figures) as described previously (3, 4). To activate TRPV4 selectively, we took advantage of the TRPV4 agonist, GSK101, to demonstrate specific activation of TRPV4 (19, 24). As shown in Fig. 2*A*, addition of 50 nM GSK101 to the split-opened CCD induced a sustained rise in $[Ca^{2+}]_i$ consistent with activation of TRPV4. The GSK101-induced time course of $[Ca^{2+}]_i$ was relatively slow, typically reaching a peak value within 1–6 min. The results are consistent with our earlier characterization of GSK101 in TRPV4-transfected HeLa cells and in the M-1 collecting duct cells which endogenously express TRPV4 (19, 25). Comparison of the responses of individual cells from a single split-opened CCD demonstrates variable responses from cell to cell that are likely reflective of the individual properties and TRPV4 expression levels of different cells from a single tubule (Fig. 2*B*). Regardless, the average response to GSK101 addition was very substantial with $[Ca^{2+}]_i$ increasing from a control value of near 90 ± 5 nM to 476 ± 35 nM at the peak (Fig. 2*E*). Further, the response to GSK101 was poorly reversible upon GSK101 washout (Fig. 2*C*) and was typically only apparent upon exposure of cells to low concentrations of GSK101 and for short exposure times, although this concept remains to be fully tested.

Finally, to provide further insight into the actions of GSK101, GSK101 was added when extracellular Ca^{2+} was removed, 0 $[Ca^{2+}]$. Indeed, in the absence of extracellular Ca^{2+}, GSK101 addition did not produce an increase in $[Ca^{2+}]_i$ (Fig. 2*D*) demonstrating that GSK101 addition led to activation of Ca^{2+} influx and not release from intracellular Ca^{2+} stores (Fig. 2*D*). These results are consistent with our earlier studies in TRPV4-HeLa cells showing that the response to GSK101 was dependent upon the presence of extracellular Ca^{2+} (19). Most importantly, in tubules isolated from animals lacking TRPV4, the response to GSK101 was completely abolished (Fig. 2, *C*, *Trace 2*, and *E*). Hence, the effect of GSK101 appears to reflect specific activation of TRPV4, with subsequent Ca^{2+} influx, with little or no component of Ca^{2+} release from stores.

Flow-induced Activation of TRPV4 in CCD and CNT—Because TRPV4 is expressed and functional within the collecting duct system, we turned to evaluate whether it may be important in flow-dependent Ca^{2+} signaling in selected tubule segments, namely the CCD and CNT. To evaluate the effect of fluid flow, the $[Ca^{2+}]_i$ responses to increases in the flow rate over the split-opened tubule luminal surface were assessed. The effect of increasing the flow rate by 10-fold, from a low control value of 1.5 ml/min to 15 ml/min (high flow or flow), through our open chamber (0.5-ml volume), was evaluated for all flow studies. As shown for the representative example in Fig. 3*A*, high flow rates induced an immediate and sustained rise in $[Ca^{2+}]_i$. After returning the flow rate to control conditions, the response to a second flow stimulus showed a similar rise in $[Ca^{2+}]_i$ with little evidence of desensitization (Fig. 3*A*).

To determine whether the flow-induced responses were in the physiological range expected for collecting duct, a few studies were performed with a defined fluid shear stress (SS) using a parallel plate chamber as done before (see Refs. 4, 26). Indeed, as shown in Fig. 3*D*, SS at 1 and 3 dynes/cm^2 induced a progressive rise in $[Ca^{2+}]_i$ with increasing SS levels. The response at 3 dynes/cm^2 was sustained and similar in magnitude to that observed in the open chamber, thereby verifying that the responses to SS in the physiological range are

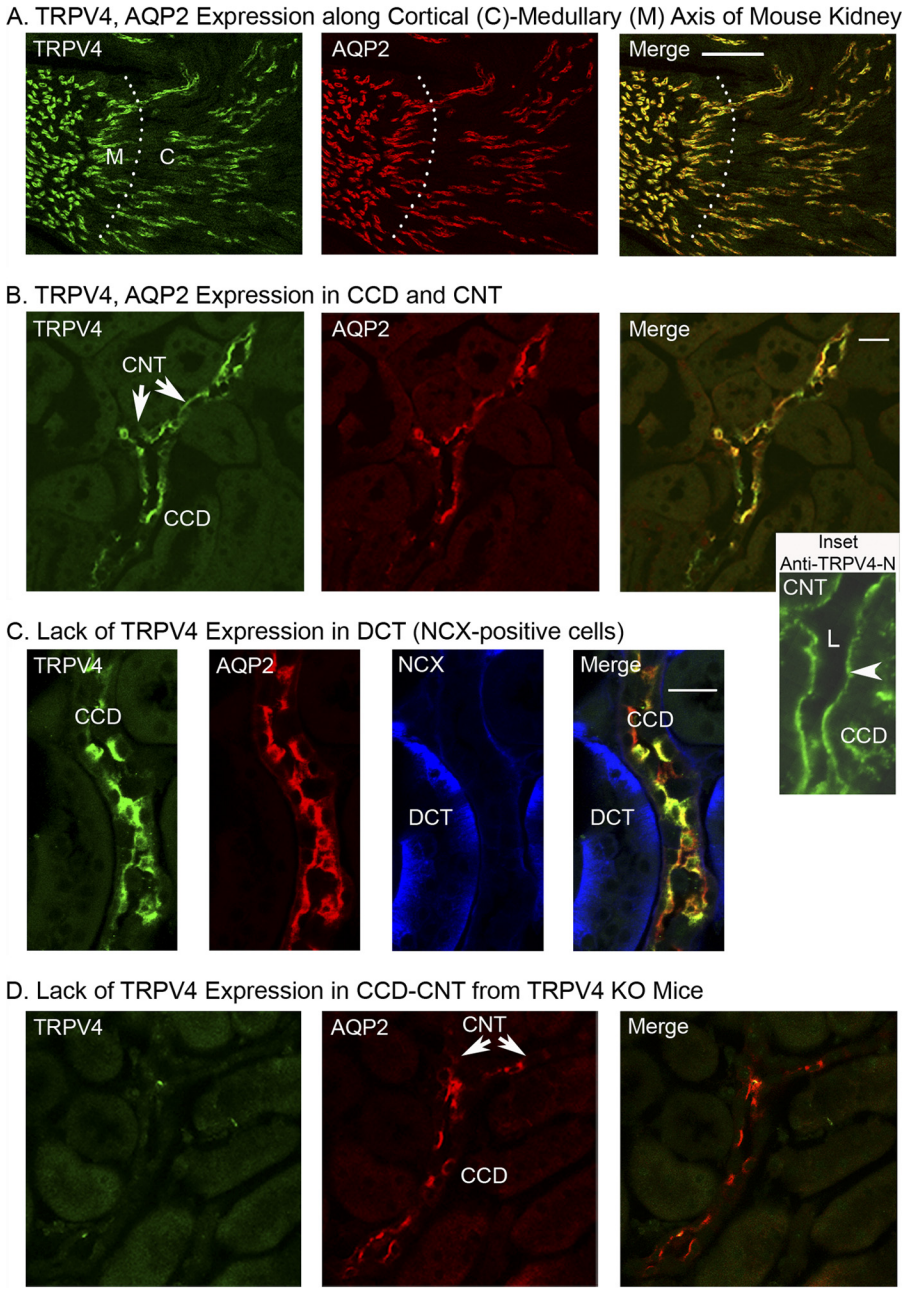

FIGURE 1. **Immunohistochemical staining of mouse kidney sections from WT (*A–C*) and TRPV4 knock-out (*D*) mice.** *A*, low magnification transverse section (30 μm) along the cortical-medullary access showing staining patterns for TRPV4 (anti-TRPV4, Cy2-labeled secondary antibody, *green*) and AQP2 (anti-AQP2 directly labeled with ATTO 550, *red*). TRPV4 expression sites co-localize with AQP2-positive tubules in both the cortex (*C*) and medulla (*M*) as evident in the *Merge* image (*yellow*), but also displayed lower staining in AQP2-negative cells (*green*). Labeling of other nephron segments was not detectable, confirming labeling by TRPV4 along the entire collecting duct system. *B*, staining of an outer cortical slice showing TRPV4 and AQP2 staining along a CCD. Note the upstream bifurcation reflecting convergence of two CNT into the CCD. TRPV4 is expressed in both CNT and CCD. The *Inset* shows a thin section (5 μm) from another kidney that is stained with a second anti-TRPV4 antibody (anti-TRPV4-N) as characterized previously (4). Note the strong staining along the apical (luminal) region of the CCD and into the apparent bifurcation (possible CNT). *L* indicates the tubule lumen. *C*, outer cortical section showing AQP2-positive segment (CNT or CCD) and an NCX-positive and AQP2-negative tubule (DCT). TRPV4 expression is apparent in the AQP2-positive segment, but not in the apparent DCT segment. *D*, cortical slice from a TRPV4 knock-out animal. Note lack of TRPV4 staining in the AQP2-positive CCD (and CNT). *, $p < 0.05$. *Scale bars*: 100 μm (*A*), 20 μm (*B*), 20 μm (*C*).

reflective of that observed with high flow in the open chamber in the current study.

Repeating the study in CCD from TRPV4 knock-out animals (Fig. 3*A*, *Trace 2*) or in the presence of the TRPV inhibitor, RuR, in CCD from WT animals (Fig. 3*B*), largely abolished the flow-induced response. On average, the flow-induced increase in $[Ca^{2+}]_i$ did not show a significant increase in CCD from WT animals, when treated with RuR, and in CCD from animals deficient in TRPV4 (Fig. 3*C*). These data provide strong evidence that TRPV4 underlies the flow-induced increase in $[Ca^{2+}]_i$, at least in CCD.

To determine whether the CNT was similarly sensitive to flow, some studies were repeated in split-opened CNT. As shown for the representative example in Fig. 4*A*, elevation of

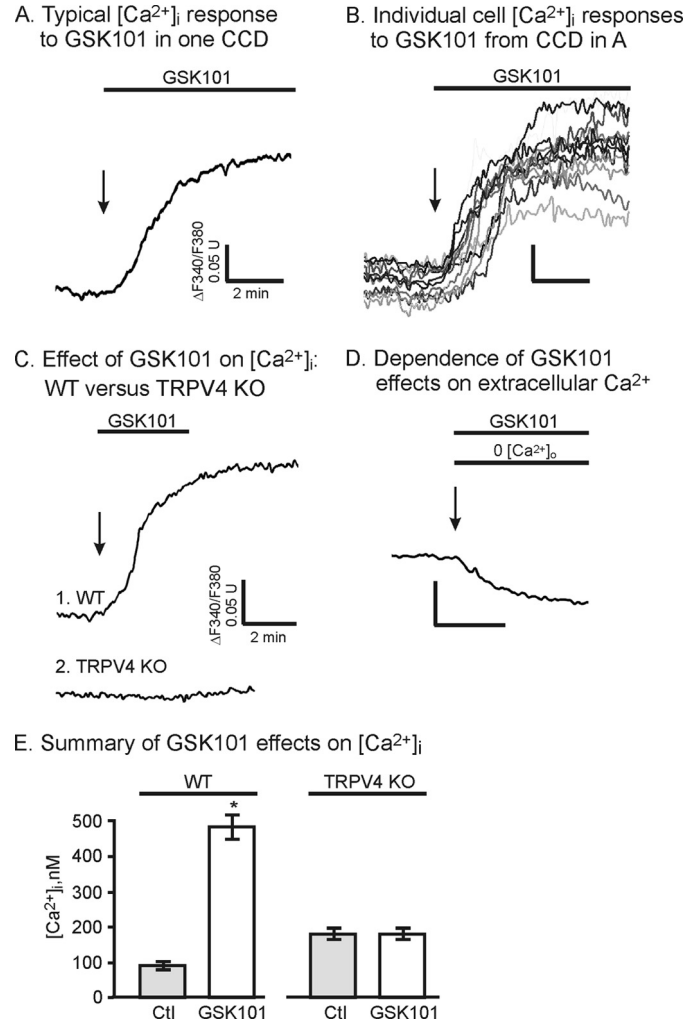

FIGURE 2. **Effect of the TRPV4 agonist, GSK101 (50 nM), on $[Ca^{2+}]_i$ in split-opened CCD.** *A*, average $[Ca^{2+}]_i$ response to GSK101 in one CCD (10 cells). *B*, response of individual cells in CCD from *A* showing variable time course and magnitude of $[Ca^{2+}]_i$ response to GSK101. *C*, $[Ca^{2+}]_i$ response to GSK101in CCD from WT (*Trace 1*) and TRPV4 KO (*Trace 2*) animals demonstrating abolition of GSK101 effect in CCD from TRPV4 KO animal. Also note limited reversibility of the GSK101 response (*Trace 1*). *D*, representative example showing removal of extracellular Ca^{2+}, 0 $[Ca^{2+}]_i$, abolishing the GSK101 response. *E*, summary of GSK101 effect on $[Ca^{2+}]_i$ in CCD from WT animals (WT, $n = 40$) and from animals deficient in TRPV4 (TRPV4 KO, $n = 14$). *, $p < 0.05$. *Error bars*, S.D.

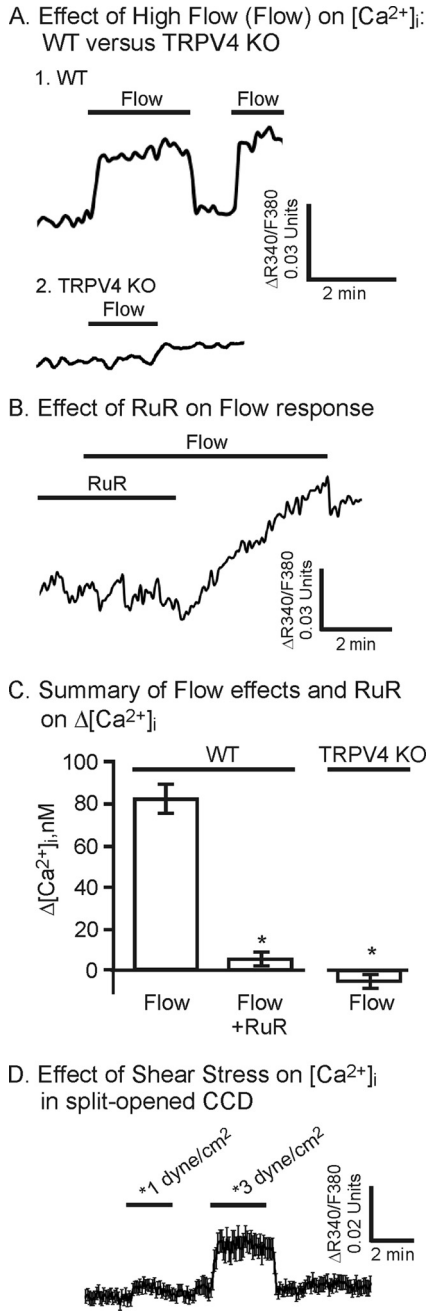

FIGURE 3. **Effect of high flow rates (*Flow*) over the luminal surface of split-opened CCD on $[Ca^{2+}]_i$.** *A*, representative traces showing $[Ca^{2+}]_i$ changes upon increasing the luminal flow by 10-fold in CCD from WT and TRPV4 deficient (*TRPV4 KO*) animals. *B*, effect of RuR (3 μM) on the flow response showing inhibition by the general TRPV channel inhibitor with subsequent recovery upon RuR washout. *C*, summary of $[Ca^{2+}]_i$ changes with high flow in CCD from WT animals showing inhibition of the response in the presence of RuR (3 μM, $n = 44$), compared with control (*Flow*, $n = 59$). The flow-induced response is abolished in CCD from TRPV4 KO animals (TRPV4 KO, $n = 35$). *Error bars*, S.D. *D*, effect of defined fluid SS on $[Ca^{2+}]_i$ of split-opened CCD. Average $[Ca^{2+}]_i$ traces (mean trace ± S.E.) showing the response to increasing SS from near 0 to 1 dyne/cm^2 and 3 dynes/cm^2 ($n = 13$). The response to higher levels of SS (3 dynes/cm^2) show a sustained increase in $[Ca^{2+}]_i$, similar to that observed to flow in the open chamber (*A*). *, $p < 0.05$.

flow rate induced a rise in $[Ca^{2+}]_i$. The magnitude and time course of the response were similar to those observed for the CCD. Likewise, addition of the TRPV4 agonist, GSK101 (50 nM), induced a potent increase in $[Ca^{2+}]_i$. The responses were similar between the CNT and CCD as evidenced in the example in Fig. 4*B*. In this study a split-opened CCD and CNT from the same tubule (the CCD and CNT at a bifurcation were both split open and studied simultaneously) were evaluated simultaneously where it is apparent that the response to GSK101 was very similar between the two segments. On average, the magnitude of the maximal responses to flow and GSK101 for CNT did not differ significantly from that observed in CCD (Fig. 4*C*).

Response to Flow in PCs versus ICs—The PCs and ICs of the collecting duct system are known to display very different properties and functions which could lead to markedly altered expression and functional levels of TRPV4. Indeed, as shown in the immunocytochemical staining images of a split-opened CCD, the expression levels of TRPV4 vary greatly among cells, particularly between PCs and ICs (Fig. 5*A*). Using AQP2 as a marker of PCs, it is apparent from the immunocytochemical

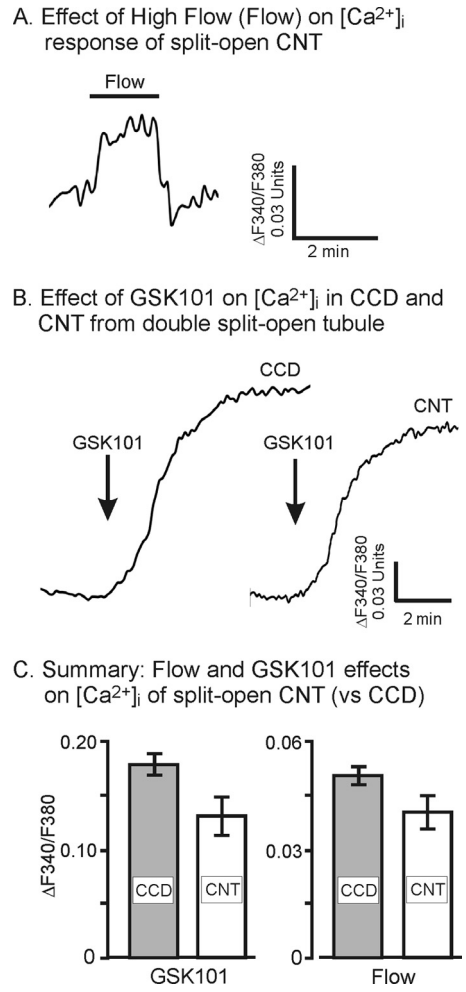

FIGURE 4. **Effect of increased flow (*Flow*) and GSK101 (50 nM) on the $[Ca^{2+}]_i$ response of split-opened CNT.** *A*, representative example showing effects of flow on $[Ca^{2+}]_i$ of CNT. *B*, representative example showing effects of GSK101 on $[Ca^{2+}]_i$ of CNT *versus* that observed in a typical CCD. The CNT and CCD are from the same split-opened tubule segment that extends from CNT to CCD. *C* summary analysis comparing the response to $[Ca^{2+}]_i$ fluorescence ratio changes with GSK101 activation in CCD ($n = 40$) and CNT ($n = 21$) and with flow in CCD ($n = 59$) and CNT ($n = 35$). *Error bars*, S.D.

staining patterns that TRPV4 is strongly expressed in AQP2-positive PCs. However, low levels of TRPV4 expression are also apparent in the APQ2-negative ICs (Fig. 5, *A* and *B*). The AQP2-negative cells were verified as ICs based on PNA labeling, a marker of ICs (Fig. 5*A*, *last panel*).

To better assess the localization of TRPV4 within PCs and ICs, we compared the apical-basal linear fluorescence intensity profile levels of TRPV4 (anti-TRPV4 staining) across PCs *versus* ICs. The intensities were normalized to the maximum intensity levels for PCs, the dominant TRPV4-expressing site. The intensity profiles for TRPV4 are shown in the graph in Fig. 5*B* for one PC and one IC as indicated in the figure. As evident from the intensity profiles, TRPV4 expression is dominant in the apical/subapical region of the PC. This is particularly apparent from the side view images in the figure (*a* and *b* sections in Fig. 5*A*). In contrast, expression levels in ICs are much lower and typically displayed dispersed distribution patterns throughout the cells as the intensity profile demonstrates.

The functional response of PCs *versus* ICs was subsequently evaluated. Both PCs and ICs responded to increased flow rates and to GSK101 addition. Typically, the IC response to flow was less than that observed in the PC (Fig. 6*A*) with the average response nearly 25% lower (Fig. 6*B*). The change in $[Ca^{2+}]_i$ was reduced from 72 ± 7 nM in PCs to 51 ± 5 nM in ICs ($p = 0.057$ for $\Delta[Ca^{2+}]_i$ data and $p < 0.05$ for $\Delta F_{340}/F_{380}$; data not shown). Likewise for the GSK101 response: the GSK101 response was less in the IC compared with PC. As shown by the example in Fig. 6*C*, addition of GSK101 at low levels induced an increase in $[Ca^{2+}]_i$ in both PCs and ICs from the same tubule, but the IC response was depressed. The mean response of the ICs was nearly 40% lower than that of the PCs (Fig. 6*D*). Hence, although TRPV4 is clearly still functional in the ICs, it appears to have a reduced activity, likely as a result of the low expression levels of TRPV4 in the ICs.

DISCUSSION

In the current study we investigated the sites of expression and function of TRPV4 in the mammalian renal collecting duct system. We provide new evidence that TRPV4 is expressed and functional within the collecting duct system. Our immunocytochemical staining patterns demonstrate strong expression of TRPV4 along the entire collecting duct, from the connecting tubule through the papillary collecting duct (Fig. 1). TRPV4 labeling was not detected with our anti-TRPV4 antibody in other segments of the nephron, including the immediate upstream segment of the CNT, the DCT (Fig. 1). Further, within the collecting duct system, TRPV4 was strongly expressed in the AQP2-positive cells, *i.e.* the PC, with strongest staining near the apical membrane (luminal membrane) and subapical region, confirming our earlier assessment (4) and that of Heller and co-workers (27). It was also shown that whereas TRPV4 co-localized with AQP2 in the subapical region of PCs, TRPV4 expression was typically further enhanced over that of AQP2 toward the apical cell membrane (Fig. 5*A*, *Merge*). Furthermore, low levels of TRPV4 expression were detected in the ICs, but the staining patterns were more diffuse (Fig. 5*B*). Finally, it is noted that the identified sites of TRPV4 expression in our study differ from that reported by Tian *et al*. (28) where their antibody demonstrated strong staining starting in the thin ascending limb and continuing along the thick ascending limb, DCT, and entire collecting duct system, particularly in the basal aspects of the IC. Why there is a difference in staining patterns is not known but likely reflects different specificities of the antibodies employed in the two studies. Our functional assessments in WT and TRPV4 KO tissue, however, are consistent with our observed pattern of staining in the current study (see below).

Our assessment of the patterns of TRPV4 localization are supported by our functional studies in split-opened CCD and CNT where we demonstrated that the selective TRPV4 agonist, GSK101, induced a potent stimulation of Ca^{2+} influx (Fig. 4). It is noteworthy that GSK101 was identified as a selective agonist of TRPV4 in a recent small molecule screening study (24). Subsequently, we (19) and others have confirmed the agonist specificity (5, 29). We now show in the current study that GSK101 activates Ca^{2+} influx in CCD, but only in CCD from WT animals and not in CCD from animals lacking TRPV4. Furthermore, the effect of GSK101 on $[Ca^{2+}]_i$ was observed to be most

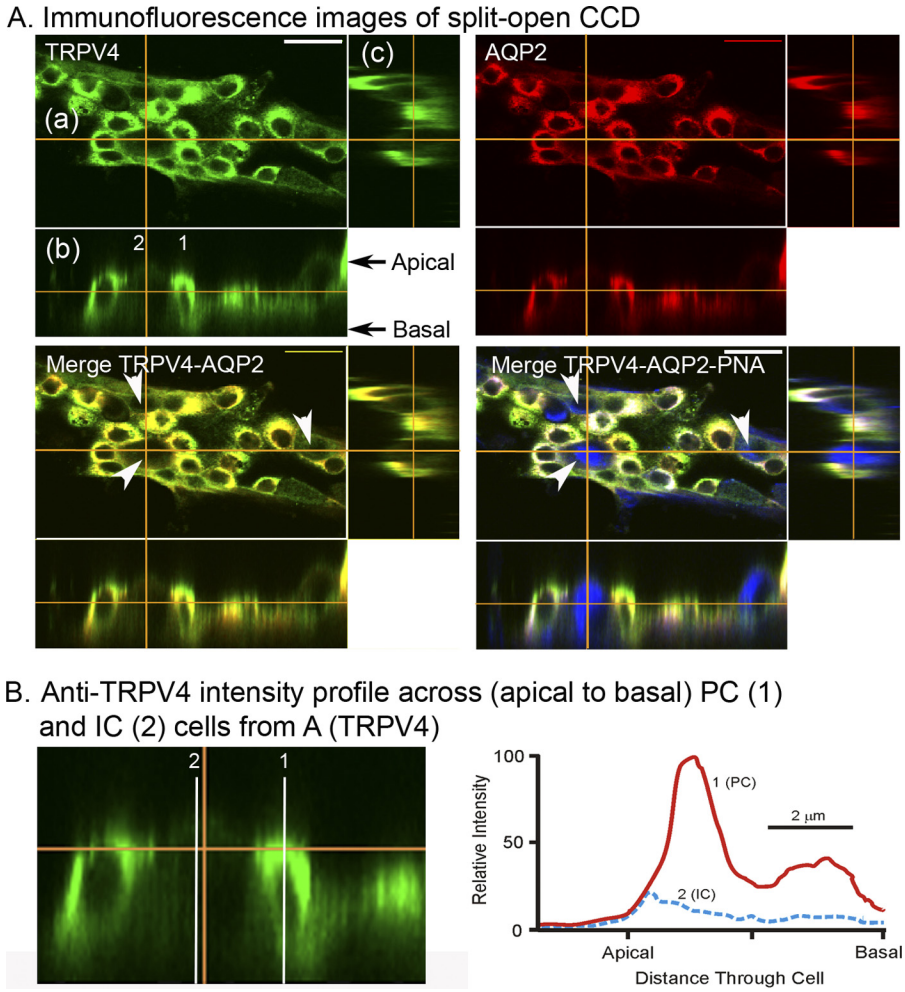

FIGURE 5. **Immunofluorescent localization of TRPV4 within split-opened CCD.** *A*, fluorescence confocal image of split-opened CCD showing localization of binding of anti-TRPV4 (*TRPV4 panel*, *green*) and anti-AQP2 (*AQP2 panel*, *red*). Each panel shows an *en face* view (*a*), a longitudinal side view (*b*), and a vertical side view (*c*). The *orange lines* indicate the plane of the image slice. The *Merge TRPV4-AQP2 panel* shows strong co-localization of TRPV4 with AQP2 reflecting expression of TRPV4 in PCs. Cells that are AQP2-negative, showing weak TRPV4 labeling, are reflective of ICs. In the *Merge TRPV4-AQP2-PNA panel*, cells are also labeled with PNA (*blue*), a marker of IC, clearly defining the AQP2-negative cells as ICs. In addition, the longitudinal side view of the *Merge TRPV4-AQP2 panel* indicates more intense labeling of TRPV4 over AQP2 at or near the luminal border, indicative of a luminal membrane function. Longitudinal side views of PCs in the *TRPV4 panel* further demonstrate strong TRPV4 binding near the apical (luminal) border and throughout the subapical region and lateral regions, with weak binding through the basal aspects of the PCs. However, ICs (two in *TRPV4 panel*) also show modest levels of TRPV4 expression throughout the apical and basal regions of the cells. *B*, expanded cross-section of the longitudinal side view from *A*, *TRPV4 panel*, showing the anti-TRPV4 intensity profiles across the PCs and ICs. Intensity profiles were obtained along the *white lines* shown in the figure for one PC (*1*) and one IC (*2*). The intensity profiles are normalized to the maximal intensity of TRPV4 in the PC (as 100). As apparent, in ICs the intensity level for TRPV4 is only 15–20% of that observed in PCs. *Scale bar*: 5 μm.

potent in PCs with an increased stimulation of $[Ca^{2+}]_i$ compared with that in ICs. These results are consistent with our immunocytochemical analysis showing strong expression of TRPV4 in PC, but weak expression in IC, as heretofore noted. Hence, the combined immunocytochemical and functional analysis point to expression of functional TRPV4 along the entire collecting duct system with strongest expression in the apical/subapical region of the PCs.

The function of TRPV4 within the kidney remains an activate area of investigation. Satlin and co-workers recently demonstrated in isolated perfused CCD from rabbit that increased perfusion flow rates induced Ca^{2+} influx (16). Furthermore, these investigators tested elevated flow rates over the luminal surface of split-opened rabbit CCD and demonstrated a sustained $[Ca^{2+}]_i$ response in both PCs and ICs. Our studies directly confirm these results in split-opened mouse CCD. In addition, we demonstrate in a parallel plate SS study that the Ca^{2+} response to physiological SS (3 dynes/cm^2) (4, 26) in CCD is similar to that observed for high flow in our open chamber, thereby verifying the physiological nature of our findings. Hence, these results directly support our studies and the role for TRPV4 in this process where we demonstrate flow-induced activation of Ca^{2+} influx in both PC and IC via a TRPV4-mediated process. Our studies further demonstrate that TRPV4 serves a similar function in the CNT (Fig. 4) implicating TRPV4 as a key flow-dependent process in the entire collecting duct system. However, the extent of this function may differ from cell type to cell type, and possibly from tubule segment to tubule segment, because it is clear in our studies that the noted alterations in TRPV4 expression between PCs and ICs lead to parallel functional alterations in the magnitude of flow- and GSK101-induced Ca^{2+} influx (compare Fig. 5 with Fig. 6). Nonetheless, this flow-dependent function may be a common control mechanism for TRPV4 because we have previously

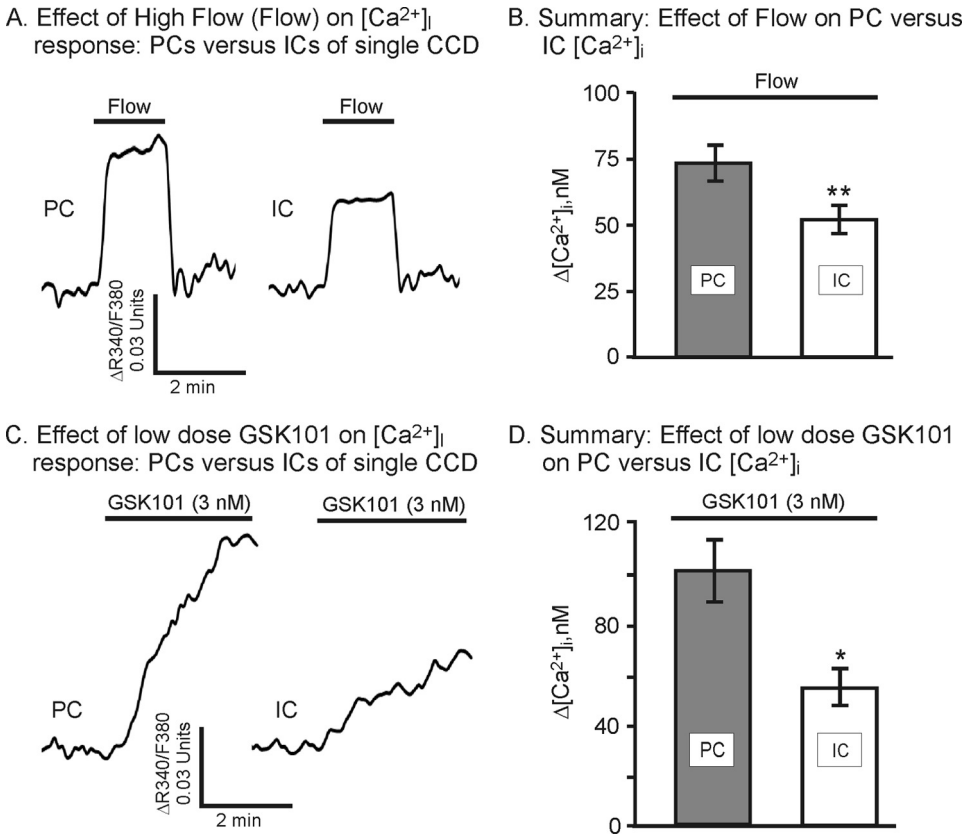

FIGURE 6. **Effect of flow (*Flow*) and GSK101 on $[Ca^{2+}]_i$ response in PC *versus* IC of split-opened CCD.** *A*, representative traces of flow on $[Ca^{2+}]_i$ in PCs and ICs. *B*, summary of the effect of flow on changes in $[Ca^{2+}]_i$ showing a marginally reduced response in IC relative to PC ($n = 34$ for PC; $n = 17$ for IC).*, $p = 0.057$ ($p < 0.05$ for $\Delta F_{340}/F_{380}$). *C*, representative traces showing the effect of low levels of GSK101 (3 nM) on $[Ca^{2+}]_i$ of PCs and ICs. *D*, summary of the effect of GSK101 on changes in $[Ca^{2+}]_i$ showing a reduced response in ICs relative to PC ($n = 32$ for PC; $n = 13$ for IC). *, $p < 0.05$.

shown a fluid SS-dependent activation of TRPV4 in M-1 cells and in TRPV4-transfected HEK cells (3, 4) as others have likewise demonstrated in certain vascular endothelial cells (5, 6, 30). Hence, TRPV4 may be central to regulating downstream effector pathways that are flow- and Ca^{2+}-dependent such as the previously noted flow-dependent K^+ secretory process of the early collecting duct segments (13, 14) as we have shown for the M-1 collecting duct cells (25). This concept is directly supported by the studies of Suzuki and co-workers where flow-dependent K^+ secretion in the mouse isolated perfused CCD is abolished in CCD isolated from TRPV4 knock-out animals (14).

Although TRPV4 would appear to play a role in flow-dependent phenomena in the collecting duct system, other channels may underlie or participate in this process. Most notable is another member of the TRP family, TRPP2, which was shown to be briefly and transiently activated by small increases in flow rates over the cell surface of mouse embryonic kidney cells (31, 32). However, in CCD the TRPP2 channel is expressed on the luminal membrane at the base of the primary cilia of the PCs, but apparently is not expressed in the ICs because they lack cilia (33, 34). However, as shown in the current study both PCs and ICs respond to increases in flow displaying a sustained increase in $[Ca^{2+}]_i$ levels, ruling out TRPP2 as the primary source of flow-induced Ca^{2+} influx. Further, it has most recently been demonstrated that TRPP2 must associate with TRPV4 to form a mechanosensitive channel (35, 36), a finding that further supports the concept of a central role for TRPV4 in mechanical sensing/transduction. Hence, it may be that TRPV4 is the dominant channel type in responding to high flow rates, such as shown in the current study, although the exact relation between these two channel isoforms or other channels in flow-induced phenomena remains to be elucidated.

The role of TRPV4 in responding to SS or fluid flow may be that of a sensor or a transducer of mechanical stresses. TRPV4 was originally coined as a "sensor" of mechanical stimuli because its activity was sensitive to osmotic cell swelling (1, 2). It is becoming apparent, however, that the channel may function more in the mode as a transducer of mechanical stresses. This is particularly evident in recent studies where it was demonstrated that mechanical activation of TRPV4 was dependent upon activation of underlying signaling pathways, including both the phospholipase A2/arachidonic acid pathways and the phospholipase C/diacylglycerol/PKC pathway (3, 9, 37–39). Indeed, activation of TRPV4 by hypotonic swelling is strongly dependent upon activation of phospholipase A2 and the production of downstream epoxyeicosatrienoic acids, such as 5′,6′-EET, where inhibition of phospholipase A2 or downstream cytochrome P450 markedly inhibits activation of TRPV4 (9, 40). Likewise, we have pointed to a role of phospholipase C, especially with SS-induced activation of TRPV4, where phospholipase C inhibition inhibits mechanical activation of TRPV4 (3). Most recently, we demonstrated a new role for purinergic signaling through the P2Y2 receptor- phospho-

lipase C pathway in CCD that may play a central role in activating TRPV4 by flow (17). Indeed, our initial studies demonstrate that ATP applied to split-opened CCD/CNT leads to activation of the P2Y2 receptor and, in turn, TRPV4. This signaling is markedly blunted in tubules from P2Y2 receptor knock-out or TRPV4 knock-out animals. Hence, TRPV4 appears to function more as a downstream transducer of mechanical stress, rather than a sensor, where it functions to transduce an upstream stress-induced signal into a change in Ca^{2+} influx and a Ca^{2+} signal.

In summary, the current study provides strong support for the concept that TRPV4 is strongly expressed in the collecting duct system of the mammalian kidney with differential expression profiles in the two cell types, the PCs *versus* ICs. TRPV4 was found to co-localize with AQP2 in the PCs with strong expression at the apical (luminal) membrane and subapical regions of the cell. Application of the selective TRPV4 agonist indicates functional channels in both the PCs and ICs, results consistent with the immunocytochemical staining patterns. Finally, TRPV4 is activated by increased fluid flow rate over the luminal cell surfaces where it appears to function as a transducer of mechanical stresses.

Acknowledgment—We thank Wolfgang Liedtke, Duke University, Durham, NC, for permission to use the TRPV4 knockout mice and Ellen A. Lumpkin, Columbia University College of Physicians and Surgeons, New York, NY, for the breeder pairs of TRPV4 knockout mice.

REFERENCES

1. Strotmann, R., Harteneck, C., Nunnenmacher, K., Schultz, G., and Plant, T. D. (2000) OTRPC4, a nonselective cation channel that confers sensitivity to extracellular osmolarity. *Nat. Cell Biol.* **2,** 695–702
2. Liedtke, W., Choe, Y., Martí-Renom, M. A., Bell, A. M., Denis, C. S., Sali, A., Hudspeth, A. J., Friedman, J. M., and Heller, S. (2000) Vanilloid receptor-related osmotically activated channel (VR-OAC), a candidate vertebrate osmoreceptor. *Cell* **103,** 525–535
3. Gao, X., Wu, L., and O'Neil, R. G. (2003) Temperature-modulated diversity of TRPV4 channel gating: activation by physical stresses and phorbol ester derivatives through protein kinase C-dependent and -independent pathways. *J. Biol. Chem.* **278,** 27129–27137
4. Wu, L., Gao, X., Brown, R. C., Heller, S., and O'Neil, R. G. (2007) Dual role of the TRPV4 channel as a sensor of flow and osmolality in renal epithelial cells. *Am. J. Physiol. Renal Physiol.* **293,** F1699–1713
5. Mendoza, S. A., Fang, J., Gutterman, D. D., Wilcox, D. A., Bubolz, A. H., Li, R., Suzuki, M., and Zhang, D. X. (2010) TRPV4-mediated endothelial Ca^{2+} influx and vasodilation in response to shear stress. *Am. J. Physiol. Heart Circ. Physiol.* **298,** H466–476
6. Hartmannsgruber, V., Heyken, W. T., Kacik, M., Kaistha, A., Grgic, I., Harteneck, C., Liedtke, W., Hoyer, J., and Köhler, R. (2007) Arterial response to shear stress critically depends on endothelial TRPV4 expression. *PLoS ONE* **2,** e827
7. Suzuki, M., Mizuno, A., Kodaira, K., and Imai, M. (2003) Impaired pressure sensation in mice lacking TRPV4. *J. Biol. Chem.* **278,** 22664–22668
8. Güler, A. D., Lee, H., Iida, T., Shimizu, I., Tominaga, M., and Caterina, M. (2002) Heat-evoked activation of the ion channel, TRPV4. *J. Neurosci.* **22,** 6408–6414
9. Vriens, J., Watanabe, H., Janssens, A., Droogmans, G., Voets, T., and Nilius, B. (2004) Cell swelling, heat, and chemical agonists use distinct pathways for the activation of the cation channel TRPV4. *Proc. Natl. Acad. Sci. U.S.A.* **101,** 396–401
10. Mizuno, A., Matsumoto, N., Imai, M., and Suzuki, M. (2003) Impaired osmotic sensation in mice lacking TRPV4. *Am. J. Physiol. Cell Physiol.* **285,** C96–101
11. Rieg, T., Vallon, V., Sausbier, M., Sausbier, U., Kaissling, B., Ruth, P., and Osswald, H. (2007) The role of the BK channel in potassium homeostasis and flow-induced renal potassium excretion. *Kidney Int.* **72,** 566–573
12. Pluznick, J. L., Wei, P., Grimm, P. R., and Sansom, S. C. (2005) BK-β1 subunit: immunolocalization in the mammalian connecting tubule and its role in the kaliuretic response to volume expansion. *Am. J. Physiol. Renal Physiol.* **288,** F846–854
13. Liu, W., Morimoto, T., Woda, C., Kleyman, T. R., and Satlin, L. M. (2007) Ca^{2+} dependence of flow-stimulated K secretion in the mammalian cortical collecting duct. *Am. J. Physiol. Renal Physiol.* **293,** F227–235
14. Taniguchi, J., Tsuruoka, S., Mizuno, A., Sato, J., Fujimura, A., and Suzuki, M. (2007) TRPV4 as a flow sensor in flow-dependent K+ secretion from the cortical collecting duct. *Am. J. Physiol. Renal Physiol.* **292,** F667–673
15. Taniguchi, J., Takeda, M., Yoshitomi, K., and Imai, M. (1994) Pressure- and parathyroid-hormone-dependent Ca^{2+} transport in rabbit connecting tubule: role of the stretch-activated nonselective cation channel. *J. Membr Biol.* **140,** 123–132
16. Liu, W., Xu, S., Woda, C., Kim, P., Weinbaum, S., and Satlin, L. M. (2003) Effect of flow and stretch on the $[Ca^{2+}]_i$ response of principal and intercalated cells in cortical collecting duct. *Am. J. Physiol. Renal Physiol.* **285,** F998–1012
17. Mamenko, M., Zaika, O., Jin, M., O'Neil, R. G., and Pochynyuk, O. (2011) Purinergic activation of Ca^{2+}-permeable TRPV4 channels is essential for mechano-sensitivity in the aldosterone-sensitive distal nephron. *PLoS ONE* **6,** e22824
18. Pochynyuk, O., Bugaj, V., Rieg, T., Insel, P. A., Mironova, E., Vallon, V., and Stockand, J. D. (2008) Paracrine regulation of the epithelial Na^+ channel in the mammalian collecting duct by purinergic P2Y2 receptor tone. *J. Biol. Chem.* **283,** 36599–36607
19. Jin, M., Wu, Z., Chen, L., Jaimes, J., Collins, D., Walters, E. T., and O'Neil, R. G. (2011) Determinants of TRPV4 activity following selective activation by small molecule agonist GSK1016790A. *PLoS ONE* **6,** e16713
20. Grynkiewicz, G., Poenie, M., and Tsien, R. Y. (1985) A new generation of Ca^{2+} indicators with greatly improved fluorescence properties. *J. Biol. Chem.* **260,** 3440–3450
21. Loffing, J., Loffing-Cueni, D., Valderrabano, V., Kläusli, L., Hebert, S. C., Rossier, B. C., Hoenderop, J. G., Bindels, R. J., and Kaissling, B. (2001) Distribution of transcellular calcium and sodium transport pathways along mouse distal nephron. *Am. J. Physiol. Renal Physiol.* **281,** F1021–1027
22. Loffing, J., Vallon, V., Loffing-Cueni, D., Aregger, F., Richter, K., Pietri, L., Bloch-Faure, M., Hoenderop, J. G., Shull, G. E., Meneton, P., and Kaissling, B. (2004) Altered renal distal tubule structure and renal Na^+ and Ca^+ handling in a mouse model for Gitelman's syndrome. *J. Am. Soc. Nephrol.* **15,** 2276–2288
23. Zaika, O., Mamenko, M., O'Neil, R. G., and Pochynyuk, O. (2011) Bradykinin acutely inhibits activity of the epithelial Na^+ channel in mammalian aldosterone-sensitive distal nephron. *Am. J. Physiol. Renal Physiol.* **300,** F1105–1115
24. Thorneloe, K. S., Sulpizio, A. C., Lin, Z., Figueroa, D. J., Clouse, A. K., McCafferty, G. P., Chendrimada, T. P., Lashinger, E. S., Gordon, E., Evans, L., Misajet, B. A., Demarini, D. J., Nation, J. H., Casillas, L. N., Marquis, R. W., Votta, B. J., Sheardown, S. A., Xu, X., Brooks, D. P., Laping, N. J., and Westfall, T. D. (2008) *N*-((1S)-1-{[4-((2S)-2-{[(2,4-dichlorophenyl)sulfonyl]amino}-3-hydroxypropanoyl)-1-piperazinyl]carbonyl}-3-methylbutyl)-1-benzothiophene-2-carboxamide (GSK1016790A), a novel and potent transient receptor potential vanilloid 4 channel agonist induces urinary bladder contraction and hyperactivity: Part I. *J. Pharmacol. Exp. Ther.* **326,** 432–442
25. Jin, M., Berrout, J., Chen, L., and O'Neil, R. G. (2012) *Cell Calcium*, in press
26. Cai, Z., Xin, J., Pollock, D. M., and Pollock, J. S. (2000) Shear stress-mediated NO production in inner medullary collecting duct cells. *Am. J. Physiol. Renal Physiol.* **279,** F270–274
27. Cuajungco, M. P., Grimm, C., Oshima, K., D'hoedt, D., Nilius, B., Mensenkamp, A. R., Bindels, R. J., Plomann, M., and Heller, S. (2006) PACSINs bind to the TRPV4 cation channel. PACSIN 3 modulates the subcellular

localization of TRPV4. *J. Biol. Chem.* **281,** 18753–18762
28. Tian, W., Salanova, M., Xu, H., Lindsley, J. N., Oyama, T. T., Anderson, S., Bachmann, S., and Cohen, D. M. (2004) Renal expression of osmotically responsive cation channel TRPV4 is restricted to water-impermeant nephron segments. *Am. J. Physiol. Renal Physiol.* **287,** F17–24
29. Xu, X., Gordon, E., Lin, Z., Lozinskaya, I. M., Chen, Y., and Thorneloe, K. S. (2009) Functional TRPV4 channels and an absence of capsaicin-evoked currents in freshly isolated, guinea-pig urothelial cells. *Channels* **3,** 156–160
30. Ma, X., Qiu, S., Luo, J., Ma, Y., Ngai, C. Y., Shen, B., Wong, C. O., Huang, Y., and Yao, X. (2010) Functional role of vanilloid transient receptor potential 4-canonical transient receptor potential 1 complex in flow-induced Ca2+ influx. *Arterioscler. Thromb. Vasc. Biol.* **30,** 851–858
31. Nauli, S. M., Alenghat, F. J., Luo, Y., Williams, E., Vassilev, P., Li, X., Elia, A. E., Lu, W., Brown, E. M., Quinn, S. J., Ingber, D. E., and Zhou, J. (2003) Polycystins 1 and 2 mediate mechanosensation in the primary cilium of kidney cells. *Nat. Genet.* **33,** 129–137
32. AbouAlaiwi, W. A., Takahashi, M., Mell, B. R., Jones, T. J., Ratnam, S., Kolb, R. J., and Nauli, S. M. (2009) Ciliary polycystin-2 is a mechanosensitive calcium channel involved in nitric oxide signaling cascades. *Circ. Res.* **104,** 860–869
33. Schwartz, E. A., Leonard, M. L., Bizios, R., and Bowser, S. S. (1997) Analysis and modeling of the primary cilium bending response to fluid shear. *Am. J. Physiol.* **272,** F132–138
34. Latta, H., Maunsbach, A. B., and Madden, S. C. (1961) Cilia in different segments of the rat nephron. *J. Biophys. Biochem. Cytol.* **11,** 248–252
35. Köttgen, M., Buchholz, B., Garcia-Gonzalez, M. A., Kotsis, F., Fu, X., Doerken, M., Boehlke, C., Steffl, D., Tauber, R., Wegierski, T., Nitschke, R., Suzuki, M., Kramer-Zucker, A., Germino, G. G., Watnick, T., Prenen, J., Nilius, B., Kuehn, E. W., and Walz, G. (2008) TRPP2 and TRPV4 form a polymodal sensory channel complex. *J. Cell Biol.* **182,** 437–447
36. Stewart, A. P., Smith, G. D., Sandford, R. N., and Edwardson, J. M. (2010) Atomic force microscopy reveals the alternating subunit arrangement of the TRPP2-TRPV4 heterotetramer. *Biophys. J.* **99,** 790–797
37. Xu, F., Satoh, E., and Iijima, T. (2003) Protein kinase C-mediated Ca^{2+} entry in HEK 293 cells transiently expressing human TRPV4. *Br. J. Pharmacol.* **140,** 413–421
38. Loot, A. E., Popp, R., Fisslthaler, B., Vriens, J., Nilius, B., and Fleming, I. (2008) Role of cytochrome P450-dependent transient receptor potential V4 activation in flow-induced vasodilatation. *Cardiovasc Res.* **80,** 445–452
39. Fan, H. C., Zhang, X., and McNaughton, P. A. (2009) Activation of the TRPV4 ion channel is enhanced by phosphorylation. *J. Biol. Chem.* **284,** 27884–27891
40. Vriens, J., Owsianik, G., Fisslthaler, B., Suzuki, M., Janssens, A., Voets, T., Morisseau, C., Hammock, B. D., Fleming, I., Busse, R., and Nilius, B. (2005) Modulation of the Ca2 permeable cation channel TRPV4 by cytochrome P450 epoxygenases in vascular endothelium. *Circ. Res.* **97,** 908–915
41. Jin, M., Berrout, J., and O'Neil, R. G. (2011) in *TRP Channels* (Zhu, M. X., ed) pp. 353–373, CRC Press, Boca Raton, FL